Carrier relaxation dynamics in self-assembled semiconductor quantum dots

H. Kurtze,[1] J. Seebeck,[2] P. Gartner,[2,3] D. R. Yakovlev,[1] D. Reuter,[4] A. D. Wieck,[4] M. Bayer,[1] and F. Jahnke[2]
[1]*Experimentelle Physik 2, Technische Universität Dortmund, 44221 Dortmund, Germany*
[2]*Institut für Theoretische Physik, Universität Bremen, 28334 Bremen, Germany*
[3]*National Institute for Materials Physics, P.O. Box MG-7, Bucharest-Magurele, Romania*
[4]*Angewandte Festkörperphysik, Ruhr-Universität Bochum, 44780 Bochum, Germany*
(Received 26 June 2009; revised manuscript received 23 October 2009; published 16 December 2009)

Systematic time-resolved pump-probe studies with independent variation in pump and probe energies in combination with time-resolved photoluminescence measurements have been used to investigate the dynamics of carrier capture and carrier relaxation in self-assembled (In,Ga)As/GaAs semiconductor quantum dots. Even for weak excitation, where carrier-carrier scattering is less efficient, the lower-energy quantum-dot states are rapidly populated, whereas for increasing delay times between pump and probe pulses residual populations in the higher quantum-dot states are found. A quantum-kinetic description of the carrier interaction with LO phonons is used for a treatment beyond perturbation theory to include polaron effects and to account also for the non-Markovian dynamics. On this level, the theory for the carrier-phonon interaction confirms fast initial carrier relaxation that becomes incomplete for longer times and results in a nonthermal carrier population in the considered low-temperature regime.

DOI: 10.1103/PhysRevB.80.235319 PACS number(s): 78.55.Cr, 78.67.Hc

I. INTRODUCTION

In recent years, relaxation processes of carriers in self-assembled quantum-dot (QD) structures with a three-dimensional carrier confinement have been attracting much interest. This topic is of direct relevance for applications in efficient light emitters that require fast carrier capture and relaxation. Related to this is the question whether the physics of carrier relaxation involving localized states with discrete energies is fundamentally different from semiconductors with a quasicontinuum of states. For the latter, it is well known that the carrier-phonon interaction and the carrier-carrier interaction lead to efficient carrier scattering. In this case, the electron and hole populations evolve toward quasiequilibrium states,[1] typically on a time scale before spontaneous recombination depletes the excited carriers.

For QDs the missing translational invariance suspends the requirement of momentum conservation; the energy conservation remains necessary—at least for times longer than those given by the energy-time uncertainty. The most simple picture to analyze scattering processes is then provided by Fermi's golden rule. On these grounds, various authors have studied the carrier-phonon interaction and predicted inefficient scattering processes between the localized states.[2,3] In the meantime, many experiments have demonstrated fast intradot carrier relaxation.[4–13] Several processes have been proposed that circumvent the so-called phonon bottleneck. A variety of carrier-carrier Coulomb scattering processes emerges from the possibilities of combining different initial and final states either within the QD or being delocated in the two-dimensional wetting layer (WL) and the bulk-like barrier. In particular, Auger-type processes describing carrier relaxation between QD states assisted by carrier redistribution in the delocalized WL states[14] as well as electron-hole scattering allowing for electron relaxation with a transfer of the excess energy to holes[15,16] have been investigated. Carrier scattering due to interaction with LA phonons is only efficient for small level spacings since the corresponding interaction matrix element rapidly decreases with increasing phonon momentum.[17]

On the other hand, extended theories beyond Fermi's golden rule have been developed. In a nonperturbative picture, the interaction of excited QD electrons and holes with longitudinal-optical (LO) phonons has been described in terms of polarons as quasiparticles.[18–20] An important implication for QD polarons is that the localized states are no longer associated with a single energy (in perturbation theory represented by the free-carrier energy). One uses spectral functions to characterize the renormalized energies; this treatment includes phonon satellites similar to the dressed states in quantum optics. The broadening of these states represents the finite quasiparticle lifetime. As a result, localized states are associated with a range of energies, which opens additional scattering channels for the carrier-phonon interaction. In Ref. 15, a self-consistent broadening of the delta function for the energy conservation within Fermi's golden rule already softens the predicted phonon-bottleneck result.

A quantum-kinetic theory generalizes this finding in two respects: (i) Polaronic broadening and phonon satellites are included in the spectral functions. (ii) Deviations from the strict energy conservation for short times and memory effects are taken into account. This approach for QD-polarons was used in Ref. 21 to predict fast carrier relaxation between QD levels due to carrier-phonon interaction despite a large mismatch of the free-carrier energies and the LO-phonon energy. For room-temperature conditions, it has been shown that a thermal equilibrium state is reached.[22] In the present investigations for cryogenic temperatures we find that the much sharper peaks in the polaronic spectral functions lead to a combination of rapid initial carrier scattering and a subsequent slow-down of the kinetics, which results in a nonthermal steady state.

To develop a consistent picture of carrier scattering processes in self-assembled QDs, we present results from time-resolved pump-probe and photoluminescence experiments,

which include systematic variations of QD parameters and excitation conditions. The results are explained in terms of both, carrier-phonon and carrier-carrier interaction.

II. EXPERIMENTAL OBSERVATIONS

The studied samples contained 10 layers of nominally undoped (In,Ga)As/GaAs QDs. By thermal annealing of different pieces of the as-grown sample, a series of QD structures with differing confinement-potential heights (taken as energy difference between the WL and ground-state emission) was obtained. For details on these samples see Ref. 23. The structures were held in an optical magnetocryostat at 10 K.

The pump-probe studies with ps-time resolution are based on two synchronized Ti:sapphire lasers with independently tunable emission wavelengths. Each laser emits 1.5 ps pulses with a repetition rate of 75.6 MHz; the temporal jitter between the two linearly polarized laser pulse trains was below 1 ps. A mechanical linear stage provided the temporal delay between pulses. The time-resolved differential transmission (TRDT) was acquired by a pair of lock-in amplified balanced photodiodes, taking the difference between the probe beam sent through the sample with and without pump illumination. As a reference excitation density P_{exc} we used $I_0=40\ \mathrm{W/cm^2}$, around which the pump density was varied, while the probe density was fixed at $I_0/30$.

A synchroscan streak camera with a S1 photocathode was used to detect the time-resolved photoluminescence (TRPL). In this configuration, only the pump laser was used for optical excitation. Spectral resolution was achieved by using interference filters with ~nm wide transmission windows, so that a time resolution of 2 ps was reached. Additionally, photoluminescence excitation (PLE) experiments were performed by using a tunable frequency-stabilized Ti:sapphire ring laser.

The top panel of Fig. 1 displays time-integrated photoluminescence (PL) spectra of a QD sample with a confinement potential of 90 meV taken at excitation densities $I_0/10$, I_0, and $10I_0$ into the GaAs barrier. In the high-excitation spectrum, emission from the confined *s*, *p*, *d*, and *f*-QD shells and the WL is seen. (Cf. corresponding labels given in the panel.) The spacing between the confined shells is approximately equidistant. This applies as well to the other studied QD confinement energies (not shown). At low excitation the *s*-shell emission is dominant, the *p*-shell emission is barely visible, and the other shells are not observable. We note that emission from the *p*-shell (albeit being very weak) is detected even at the lowest possible excitation powers $\sim I_0/100$, for which the average occupation can be estimated to be <0.05. From this we conclude that in all cases, some carrier population remains in the *p*-states long enough that it contributes to spontaneous recombination.

Typical examples for the time evolution of the differential transmission (DT) signal at the *s*-shell are shown in Figs. 1(b) and 1(c). In all cases, the fast rise of the signal indicates rapid buildup of ground-state population after pump pulse action. Rise times in the ps range are observed, almost independent of the confinement potential height when exciting into the GaAs barrier (b), and also nearly independent of the

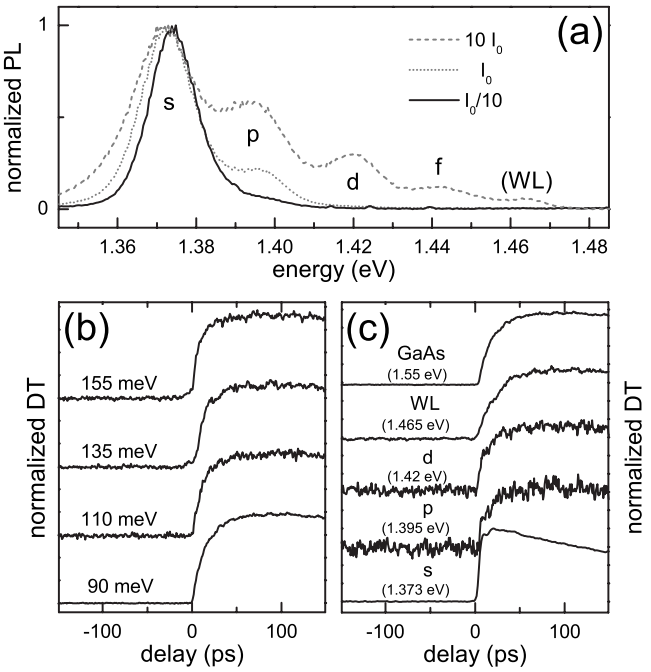

FIG. 1. (a): Time-integrated photoluminescence spectra recorded for pump intensities $I_0/10$ (solid line) I_0 (dotted line) and 10 I_0 (dashed line). The spectra were obtained for pumping into GaAs at 1.55 eV energy and a QD sample with 90 meV confinement potential. The other panels give the time evolution of the time-resolved differential transmission mapping the s-shell population vs pump-probe delay. (b): Influence of the QD confinement potential heights. (c): Various spectral positions of the pump pulse at the QD-shells, WL, and GaAs barrier interband transitions. In (b) the excitation is into GaAs at 1.55 eV; for (c) a QD sample with 90 meV confinement was used. In both cases, the pump densities correspond to I_0. (For clarity, curves are shifted vertically.)

pump excitation energy (c). In the latter case, small variations of the rise time can be attributed to different carrier transfer conditions. While ground-state filling under resonant and quasi-resonant excitation within the confined QD-shells is determined by carrier relaxation only, above barrier excitation is also accompanied with carrier capture. We find that excitation into the WL leads to slightly longer rise times due to smaller carrier capture rates than for excitation into the GaAs matrix surrounding the QDs [as reflected by the transients shown in Fig. 1(c)]. This difference may be related to carrier localization effects in the WL. However, the overall weak dependence of the rise times on the confinement potential and pump energy indicates that the relaxation is independent of the energy, which the carriers need to release to arrive in the ground states.

More insight into the temporal evolution of the carrier distribution can be obtained from experiments, in which the pump pulse excites the GaAs barrier and the transmission changes are recorded in a broad range of energies covering the interband optical transitions of the QD and WL states. Figure 2(a) shows the resulting contour plot, where the vertical (horizontal) axis provides pump-probe delay (probe energy). To record these time evolutions, we used a low pump intensity of $I_0/10$. The time-integrated PL for this excitation

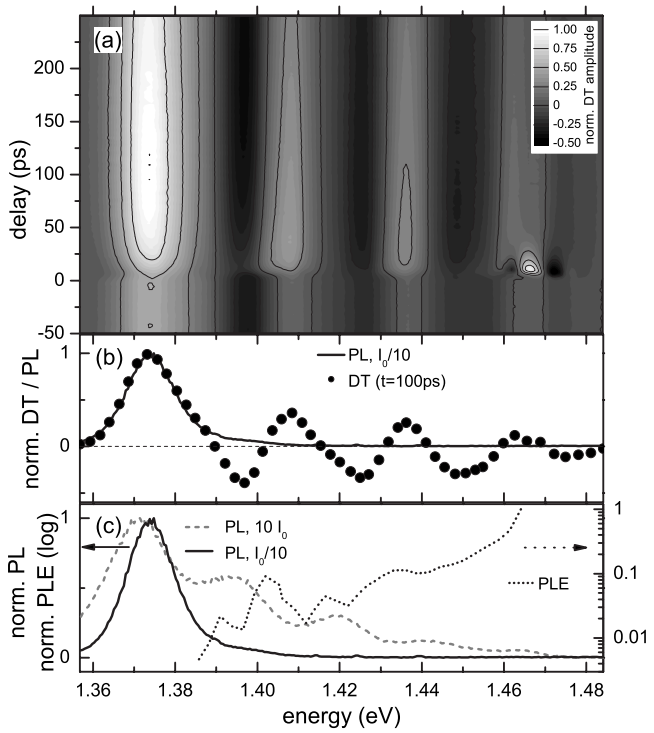

FIG. 2. (a) Contour plot of the differential transmission vs. probe energy and pump-probe delay. Panel (b) gives the DT values of the transients at $t=100$ ps delay (scattered dots). The solid line shows time-integrated PL, obtained under same pump conditions using excitation into GaAs at 1.55 eV with $I_0/10$. For comparison, spectra of PL under high and low excitation densities ($10I_0$, dashed line; $I_0/10$, solid line) and PLE (dotted line, $\log_{10}$ scale) are given in the lower panel (c). The figures were obtained on a QD sample with 90 meV confinement potential.

condition is shown in panel (b) by the black solid line. The average exciton occupation per QD is significantly below unity per excitation cycle, as estimated from comparison of a series of PL spectra at various excitation densities.

In Fig. 2(a) we observe fast rises of the DT due to pump action within a few tens of ps over the whole energy rage scanned by the probe beam. At these early times the DT is approximately equidistantly modulated, reflecting the confined shell structure. Panel (b) of Fig. 2 shows the corresponding DT values at $t=100$ ps delay (scattered dots). In contrast to the PL spectra (where no substantial emission of the excited states is found), significant DT changes are observed also for the excited states. From Fig. 2(a) it is evident, that these changes persist also to much longer times. The DT signal alone does not allow us to distinguish whether the states associated with the corresponding optical transitions are populated with electrons, holes, or both. Additional information can be obtained from PL since both, electrons and holes are required to obtain photon emission. We conclude that only the *s*-shell exhibits simultaneous population with electrons and holes. The DT signals at higher energies are most likely due to exciton complexes with QD-confined electrons in the excited states, as suggested by the large level splittings in Fig. 2(a) (see below). Since the level splitting for the holes is considerably smaller than for electrons, one expects much faster hole relaxation, so that at this delay time holes most likely occupy the ground state mostly.

A closer comparison reveals that the low-excitation DT level spacing [as shown by the scattered dots in Fig. 2(b)] is considerably larger than in high-excitation PL [dashed line in panel (c)]. Qualitatively similar results have been obtained for samples with other confinement energies. We attribute deviations in the high-excitation PL to many-body Coulomb interactions among the excited carriers, while in DT for the used pump power the observed level structure is closer to the one of the unexcited QDs.

These assignments are supported by PLE experiments. Results for the ground-state emission detected at 1.373 eV are shown in Fig. 2(c) on logarithmic scale. The high energy side of the PLE spectrum ($E>1.44$ eV) is dominated by the strong WL absorption. Energetically below discrete features are observed, which can be assigned to QD-confined levels. Two broad features appear whose energies agree well with those of the positive DT features. Small differences may be related with different Coulomb interaction energies for electrons and holes in the same states (as in PLE) and in different states (as may occur in DT).

Furthermore, there is a substantial difference between DT in zero- and in higher-dimensional systems. The presence of a single carrier or an electron-hole pair in a QD prevents absorption at the free-transition energies, while it enables absorption due to renormalized states, as the Coulomb interaction of optically excited carriers with resident carriers leads to the formation of multiexciton complexes (mostly at lower energy). Hence, shifted absorption lines are facilitated, leading to the negative DT signals which are clearly visible in Figs. 2(a) and 2(b).

The positive DT signals can be characterized additionally by applying an external magnetic field in Faraday geometry, i.e., parallel to the sample growth and beam axes. (Detailed results are shown in Appendix A.) For the DT signals observed around 1.37, 1.41, and 1.435 eV, these experiments reveal *s*, *p*, and *d*-like orbital angular momentum splittings,[24] respectively, verifying their origin in QD-confined states. Thus, the DT signals in Fig. 2 are confirmed to represent significant populations in higher states. As the average exciton occupation per QD is well below unity, these populations cannot be traced to state filling effects in lower shells which prevent relaxation due to Pauli blocking. Apparently the data indicate effective scattering channels at early times after the pump, however, later on they hint at a carrier distribution that is characterized by incomplete electron relaxation.

An additional feature of the experimental DT signal are components that persist much longer than the spontaneous recombination time and even outlast the repetition time (13.2 ns) of the experiment. This is seen in Fig. 2(a) for negative delay times. A substantial contribution of the corresponding ground-state carrier population is due to dark states, in which the spin configuration of electrons and holes prevents radiative recombination. The required spin-flip processes are very unlikely on a ns time scale. Additional measurements were performed, where a magnetic field was applied perpendicular to the incident pump and probe beams (Voigt configuration). The carriers react to this perturbation with a precession of the carrier spins around the field.[25] As a consequence the bright

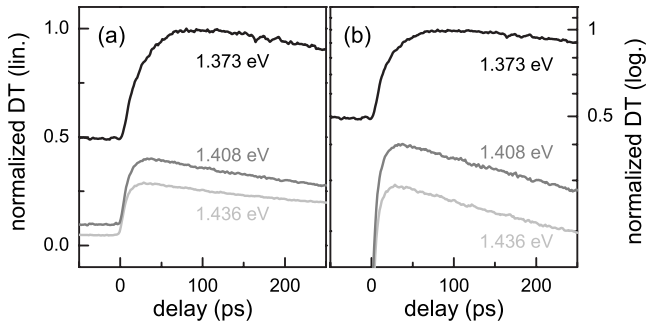

FIG. 3. Differential transmission in linear [panel (a)] and logarithmic [$\log_{10}$, panel (b)] representation for the three shells *s*, *p*, and *d* from panel (a) in Fig. 2 under the same experimental conditions. Probe energy as labeled.

and dark states mix, leading to a fast decay of the populations of electrons and holes in the same shell. This is confirmed by a reduction of the normalized DT signal to significantly lower values, when applying the magnetic field (see Appendix B). However, even under these conditions a positive DT signal remains for the excited shells over time scales exceeding the pulse repetition time, confirming that the population in higher states cannot be ascribed to Pauli-blockings from lower energy shells.

To obtain further insight into the relaxation dynamics, Figs. 3(a) and 3(b) show the time evolution of the DT signals recorded at the shell transition energies for optical excitation into the barrier states with intensity $I_0/10$. For early times after the excitation we find an almost simultaneous population of the QD shells. The maximum of the DT signal is obtained at about 30, 40, and 80 ps for the *d*, *p*, and *s*-transition, respectively. When the *d* and *p*-shell signals reach their maxima, already a significant *s*-shell response is obtained. In this respect, our experimental results deviate from the cascaded population dynamics observed in Ref. 9. The logarithmic representation of the data in Fig. 3(b) reveals that after the rapid onset of the signals only a small contribution due to further carrier redistribution between the QD shells occurs. The continuous small increase of the s-shell signal up to ~80 ps indicates a further growing carrier population due to scattering of carriers from the higher QD states or directly from the WL or barrier states. For delay times larger than 50 ps the decay of the higher shells follows nearly the same exponent, reflecting net population loss with time constants of ~0.4 ns corresponding to the PL decay time. Hence, for the d- and p-shell, after 50 ps additional in-scattering of carriers from higher-lying states is approximately compensated by out scattering into lower states, from which only the s-shell has a net benefit.

As mentioned, in the discussed DT signal one cannot distinguish, whether population effects are due to electrons, holes, or both. Complementary information can be obtained from the PL measurements, since electron-hole pairs need to be present in the respective states for radiative recombination. In the past, a rapid onset of the QD TRPL after optical excitation of the barrier states has been reported.[4,6,8,10,26,27]

Also for the present sample and excitation conditions, a fast rise of the TRPL signal at the *s*-shell on a ps time scale

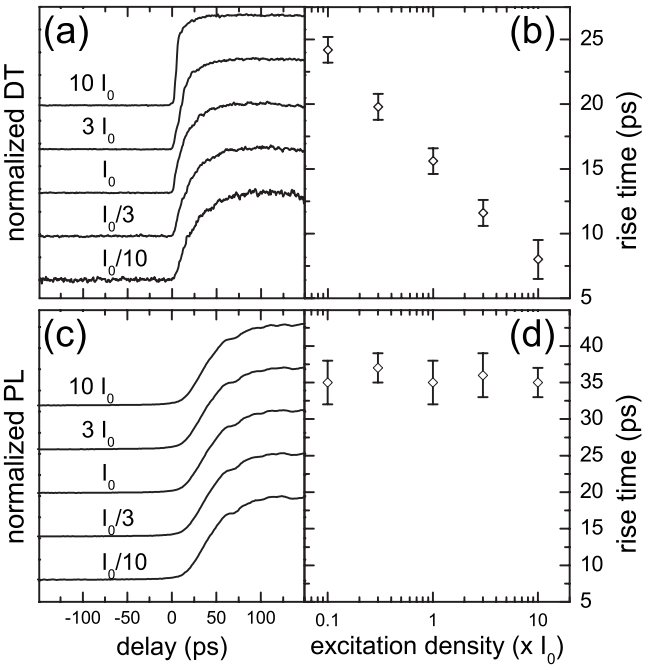

FIG. 4. Temporal evolution of the time-resolved differential transmission signal (a) and extracted rise time (b) for various excitation intensities I_0. Panels (c) and (d) show corresponding results for time-resolved photoluminescence measurements. (All panels: QD-confinement 90 meV, excitation into GaAs at 1.55 eV.)

is verified. The *s*-shell DT as well as the corresponding PL signal are displayed in Fig. 4 for different pump intensities and above barrier excitation. Even at the weakest pump excitation, in both cases a fast rise of the signal is observed, which requires a rapid population buildup for electrons as well as holes. Remarkably, the rise time of the TRPL signal is independent of the excitation density. This indicates the importance of phonon scattering processes in the carrier relaxation: For weak excitation, the corresponding scattering time (introduced in relaxation-time approximation[28]) is independent of the excitation density. In contrast, the DT measurements are clearly influenced by Coulomb-scattering processes, as can be seen from the shortening of the rise time with increasing carrier density.

Theoretical investigations of Coulomb scattering for self-assembled QD systems, which include Auger-like processes as well as electron-hole scattering, generally predict a shortening of capture and relaxation times with increasing carrier density.[28] However, the role of various processes depends on the particular excitation conditions. For optical excitation of the WL or barrier states, with increasing excitation density the availability of scattering partner grows, facilitating rising capture and relaxation rates of carriers into and between the QD states, as indicated in Fig. 4. On the other hand, for weak excitation (with the number of generated electron-hole pairs falling substantially below the QD number), in Ref. 9 it has been pointed out that one has to distinguish (mainly) between QDs, in which electron-hole pairs are captured and those receiving only single electrons and holes. For the former case assuming that the electron is not directly captured to the ground state irrespective of the excitation density

electron-hole scattering is possible. With the usually shallower hole confinement, one expects electron relaxation, in which the excess energy is transferred to the hole. In the latter case of individually captured carriers, Coulomb scattering is suppressed, giving rise to long-lived population. Nevertheless, Coulomb scattering does not dissipate kinetic energy from the carrier system. This is, however, a prerequisite to find both, electrons and holes in the QD ground states. We conclude that for the TRPL in Figs. 4(c) and 4(d) the required carrier-phonon interaction limits the observed rise time, while for the TRDT in Figs. 4(a) and 4(b) the Coulomb-scattering is responsible for the shorter rise time with increasing carrier densities.

III. THEORETICAL ANALYSIS

In the light of the experimental findings, we address the question, whether the emission of LO phonons is able to provide the necessary energy dissipation in QD systems. In this respect, we focus on the temporal evolution of the electrons due to carrier-LO-phonon scattering, as the DT results suggest incomplete electron relaxation. Only the perturbative treatment of the carrier-phonon interaction predicts the phonon bottleneck; the polaron picture allows carrier relaxation due to LO-phonon emission even if the energy conservation in terms of free-carrier states is not met. As mentioned in the introduction, this is the result of the quasiparticle picture where an interacting state is associated with a range of energies, in addition to non-Markovian effects that violate the energy conservation on short time scales.

In order to quantify the role of polarons for carrier relaxation in the analyzed self-assembled QDs, we evaluate a quantum-kinetic theory described in Refs. 21 and 22 for the low-temperature regime studied in this paper. We consider a QD with s, p, and d-shells, where the parameters are chosen in accordance with the PL spectra, discussed above in Fig. 1(a), but omitting the f-shell, which is observed in the experiment. Assuming a cylindrical symmetry and parabolic in-plane confinement, the p-shell is twofold degenerate ($p_\pm$) and the d-shell is threefold degenerate ($d_\pm, d_0$).

The results for optical excitation in the WL are given in Fig. 5(a) and show efficient transfer of carriers from the WL into the QD states in the early stage of the time evolution. As in the experimental results, we do not observe a cascaded relaxation but rather a simultaneous population of the QD states. In the subsequent time evolution, we find a slowdown of the population changes until a steady state is reached. These quantum-kinetic findings show that perturbative arguments should not be used to exclude carrier capture and relaxation due to the interaction with LO phonons.

Superimposed to the time evolution of population functions in Fig. 5(a) are Rabi-like oscillations which are similar to those encountered in quantum optics but here arising from the coupling with LO phonons[18] rather than from light-matter interaction. In the experimental results, these oscillations are concealed by inhomogeneous broadening.

To reveal the long-time properties of the relaxation processes more clearly, spontaneous recombination processes have not been included in the calculation. We use a single-

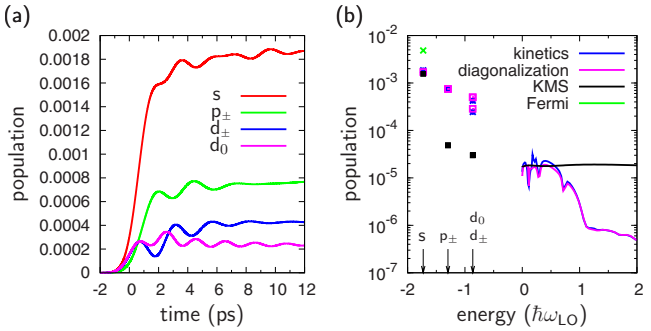

FIG. 5. (Color online) Temporal evolution of the QD population for electrons due to carrier-LO-phonon scattering after optical pulse excitation into the WL [panel (a)] and steady-state electron population compared to the thermal carrier distribution [$\log_{10}$ scale, panel (b)]. The discrete values for negative energies correspond to the localized QD states (s, $p_\pm$, $d_\pm$, d_0) and positive energies represent WL states.

time formulation of the quantum-kinetic theory, which allows us to follow the time evolution numerically until a steady state is reached. Alternatively, one can determine the stationary solution of the kinetic equations as an eigenvector corresponding to the zero eigenvalue of a transition rate matrix, which is obtained by diagonalization of the latter. With our second method, which also takes into account the quasiparticle spectral functions, the stationary solution does not depend on particular initial conditions but only on the density of excited carriers, the lattice temperature, and the QD parameters. The results presented in Fig. 5(b) show good agreement between the steady state results obtained by explicitly following the time evolution and that given by the diagonalization method. This also confirms that one has indeed reached the long-time limit of the kinetics.

A fundamental question to the quantum-kinetic theory is whether the system approaches the thermal equilibrium or evolves into a different steady state. The thermal equilibrium is described by the Fermi function only in the absence of interaction. A generalization to interacting systems is given by the Kubo-Martin-Schwinger (KMS) formula that includes the renormalized quasiparticle properties, see Ref. 22 and references therein. For the strong coupling regime of QD carriers and LO phonons, one expects significant modifications. It has been shown, that, in case of the interaction with LO-phonons at room-temperature conditions, the time evolution of the quantum-kinetic theory reaches the thermal equilibrium state of the interacting system.[22]

For the present low-temperature situation (10 K), the steady-state results of the time evolution and from the alternative diagonalization method are compared in Fig. 5(b) with the equilibrium-state population of the interacting system (KMS) and the Fermi-function calculated with free-carrier energies. In all cases, the population functions correspond to the same carrier density. The Fermi function is shown only for the s-shell, since all the other states in a free-carrier picture would be practically empty at this temperature. This is not the case for the thermal distribution with the interaction included. A comparison of the steady state solution of the quantum-kinetic theory (time evolution and diagonalization)

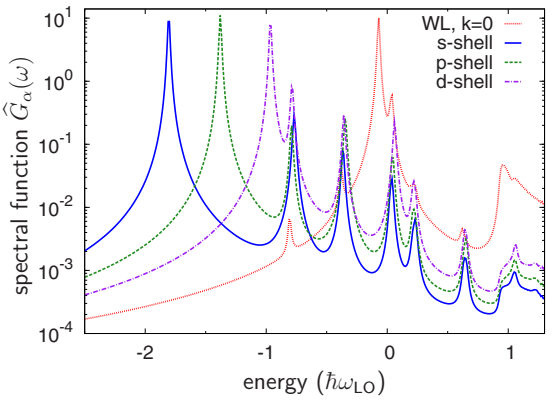

FIG. 6. (Color online) Electron spectral function for the QD *s*, *p*, and *d*-states and for the band edge of the WL ($\log_{10}$ scale). The evolution of the quantum-kinetic theory has been performed in the time-domain where the spectral functions have very slowly decaying components at 10 K. To facilitate the shown Fourier transform (this has no influence on the calculated population dynamics) a broadening of 2 ps has been added. For efficient carrier scattering in the stationary regime due to LO-phonon emission/absorption, the spectral functions of the initial (i) and final (f) state require a large overlap $\int d\omega \hat{G}_i(\omega \mp \omega_{LO})\hat{G}_f(\omega)$. The short-time evolution corresponds to an incomplete Fourier transform regarding the spectral functions resulting in substantially increased broadening.

with the KMS result shows that the stationary distribution is not thermalized. More explicitly, the *s*-state population is rather close to the KMS value, but the *p* and *d*-states are overpopulated at the expense of the higher WL states. Hence, the quantum-kinetic theory for carrier interaction with LO phonons at low temperatures reveals two distinct properties: the rapid redistribution of carriers in the initial stage is confronted with a reduction of the scattering rates at later times in a way that prevents the system from reaching thermal equilibrium.

This result has to be compared to the experimental data from Fig. 2(b). As discussed, the excited state populations shown there most likely correspond to that of electrons as calculated. Excited state hole populations which would result in corresponding PL emission most likely do not occur as the narrow energy level splitting in the valence band allows efficient relaxation into the ground state. From the data we expect ratios of confined shell populations of 1:0.35:0.25, comparing the *s*, *p*, and *d*-shells. These ratios in the quantum kinetic theory are 1:0.4:0.35, which is in reasonable agreement with experiment.

The explanation for the nonthermalized behavior relies on the spectral properties of the polarons for low lattice temperatures. Indeed, in this case the polaron spectral function (corresponding to the density of states for the interacting system) exhibits much sharper peaks at 10 K (Fig. 6) than at room temperature (Fig. 4 in Ref. 21). The low-temperature result is reminiscent of the free-carrier case and suggests the appearance of a reduced scattering efficiency by requiring a definite phononic energy to produce the transition. But for the early time regime, when a sharp energy conservation has not yet built up, fast scattering channels are still open.

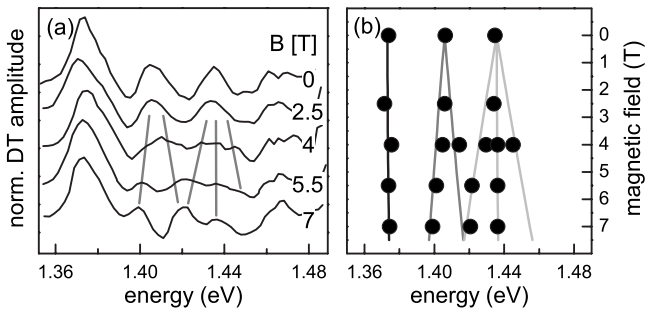

FIG. 7. (a) Results from time-resolved differential transmission experiments for 3 ns delay and different magnetic field strengths applied in Faraday configuration. For clarity, the curves are shifted vertically. The graphs were obtained for pumping into GaAs at 1.55 eV with I_0 on a QD sample with 90 meV confinement potential. Panel (b) shows the energies of the DT features as obtained from (a) vs magnetic field. Lines are guides to the eye.

IV. CONCLUSION

Ultrafast differential transmission changes for the QD resonances combined with the almost instantaneous onset of photoluminescence after optical pulse excitation into the barrier states indicate fast carrier capture and relaxation for the QD states, but also require the presence of an energy dissipation mechanism. It was shown that the carrier interaction with LO phonons provides such a mechanism also for QD systems. The seemingly contradicting observation of fast initial carrier redistribution and incomplete thermalization is consistent with a nonperturbative quantum-kinetic description of the physical processes.

ACKNOWLEDGMENTS

We gratefully acknowledge financial support from the DFG and a grant for CPU time at the Forschungszentrum Jülich (Germany).

APPENDIX A: IDENTIFICATION OF THE QD SHELL STRUCTURE

The positive DT signals of Figs. 2 and 3 can be characterized by applying an external magnetic field in Faraday geometry as shown by DT spectra for a fixed delay time in Fig. 7(a). We used the experimental conditions discussed in Sec. II with excitation density I_0. DT amplitudes for a delay time $t=100$ ps, as given in Fig. 2(b), show multiexcitonic contributions blurring somewhat the orbital angular momentum splittings. Thus, the panel shows DT amplitudes at a larger delay time of $t=3$ ns when multiexcitons have decayed radiatively. Additionally, panel (b) gives the energies of the DT features versus magnetic field. As the data indicate, the zero magnetic field DT components at 1.37, 1.41 and 1.435 eV reveal *s*, *p*, and *d*-like orbital angular momentum splittings, respectively. This verifies that the components originate from the corresponding QD-confined states.

APPENDIX B: INFLUENCE OF DARK EXCITON POPULATION

Another question is whether the occupation of higher-lying states can be attributed to Pauli-blocking effects. Particularly at longer delay times a significant fraction of the QD ground-state carrier population at $B=0$ can be traced to optically inactive ("dark") exciton states with total angular momentum $M=\pm 2$. In presence of magnetic fields perpendicular to beam and sample growth axes bright and dark stares mix which leads to a significant reduction of the exciton ground-state population. This is confirmed by experimental DT data in Fig. 8(a), recorded for the same experimental conditions as in Fig. 7 except for Voigt configuration. Increasing magnetic field strength leads to a decrease of the ground-state population around 1.37 eV. The corresponding transients for the ground-state signal are given in panel (b). In contrast, the population of the DT components at 1.41 and 1.435 eV are significantly less affected by the applied fields.

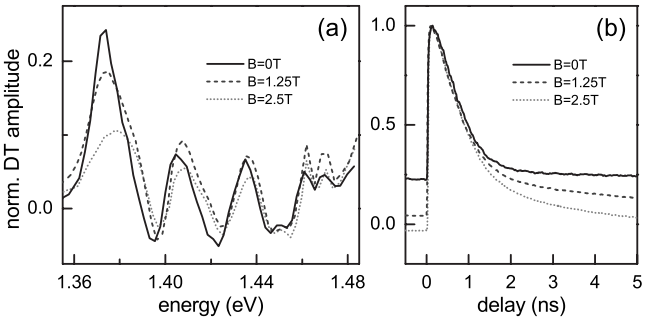

FIG. 8. DT values at a fixed delay [$t=3$ ns, panel (a)] and TRDT transients at 1.37 eV probe energy (b) for different magnetic field strengths in Voigt configuration. Other experimental conditions as in Fig. 7.

As panel (a) shows, their amplitudes remain almost unchanged with increasing fields.

[1] J. Shah, *Ultrafast Spectroscopy of Semiconductors and Semiconductor Nanostructures* (Springer-Verlag, Berlin, 1999).
[2] U. Bockelmann and G. Bastard, Phys. Rev. B **42**, 8947 (1990).
[3] H. Benisty, C. M. Sotomayor-Torres, and C. Weisbuch, Phys. Rev. B **44**, 10945 (1991).
[4] B. Ohnesorge, M. Albrecht, J. Oshinowo, A. Forchel, and Y. Arakawa, Phys. Rev. B **54**, 11532 (1996).
[5] T. S. Sosnowski, T. B. Norris, H. Jiang, J. Singh, K. Kamath, and P. Bhattacharya, Phys. Rev. B **57**, R9423 (1998).
[6] D. Morris, N. Perret, and S. Fafard, Appl. Phys. Lett. **75**, 3593 (1999).
[7] Y. Toda, O. Moriwaki, M. Nishioka, and Y. Arakawa, Phys. Rev. Lett. **82**, 4114 (1999).
[8] S. Marcinkevičius, A. Gaarder, and R. Leon, Phys. Rev. B **64**, 115307 (2001).
[9] J. Urayama, T. B. Norris, J. Singh, and P. Bhattacharya, Phys. Rev. Lett. **86**, 4930 (2001).
[10] F. Quochi, M. Dinu, N. H. Bonadeo, J. Shah, L. N. Pfeiffer, K. W. West, and P. M. Platzman, Physica B **314**, 263 (2002).
[11] E. Péronne, F. Fossard, F. H. Julien, J. Brault, M. Gendry, B. Salem, G. Bremond, and A. Alexandrou, Phys. Rev. B **67**, 205329 (2003).
[12] F. Quochi, M. Dinu, L. N. Pfeiffer, K. W. West, C. Kerbage, R. S. Windeler, and B. J. Eggleton, Phys. Rev. B **67**, 235323 (2003).
[13] E. W. Bogaart, J. E. M. Haverkort, T. Mano, T. van Lippen, R. Nötzel, and J. H. Wolter, Phys. Rev. B **72**, 195301 (2005).
[14] U. Bockelmann and T. Egeler, Phys. Rev. B **46**, 15574 (1992).
[15] I. Vurgaftman, Y. Lam, and J. Singh, Phys. Rev. B **50**, 14309 (1994).
[16] A. L. Efros, V. A. Kharchenko, and M. Rosen, Solid State Commun. **93**, 281 (1995).
[17] E. B. Flagg, J. W. Robertson, S. Founta, W. Ma, M. Xiao, G. J. Salamo, and C. K. Shih, Phys. Rev. Lett. **102**, 097402 (2009).
[18] T. Inoshita and H. Sakaki, Phys. Rev. B **56**, R4355 (1997).
[19] S. Hameau, J. N. Isaia, Y. Guldner, E. Deleporte, O. Verzelen, R. Ferreira, G. Bastard, J. Zeman, and J. M. Gérard, Phys. Rev. B **65**, 085316 (2002).
[20] V. Preisler, T. Grange, R. Ferreira, L. A. de Vaulchier, Y. Guldner, F. J. Teran, M. Potemski, and A. Lemaitre, Phys. Rev. B **73**, 075320 (2006).
[21] J. Seebeck, T. R. Nielsen, P. Gartner, and F. Jahnke, Phys. Rev. B **71**, 125327 (2005).
[22] P. Gartner, J. Seebeck, and F. Jahnke, Phys. Rev. B **73**, 115307 (2006).
[23] A. Greilich, M. Schwab, T. Berstermann, T. Auer, R. Oulton, D. R. Yakovlev, M. Bayer, V. Stavarache, D. Reuter, and A. Wieck, Phys. Rev. B **73**, 045323 (2006).
[24] S. Raymond *et al.*, Phys. Rev. Lett. **92**, 187402 (2004).
[25] M. Bayer, O. Stern, A. Kuther, and A. Forchel, Phys. Rev. B **61**, 7273 (2000).
[26] T. Berstermann *et al.*, Phys. Rev. B **76**, 165318 (2007).
[27] G. J. Beirne, M. Reischle, R. Rossbach, W. M. Schulz, M. Jetter, J. Seebeck, P. Gartner, C. Gies, F. Jahnke, and P. Michler, Phys. Rev. B **75**, 195302 (2007).
[28] T. R. Nielsen, P. Gartner, and F. Jahnke, Phys. Rev. B **69**, 235314 (2004).